ORIGINAL RESEARCH

Polyethyleneimine/activated carbon paper-based material for low-concentration hexavalent chromium removal

Tianliang Gao · Chuanshan Zhao · Sha Wang · Xia Li · Qijun Ding

Abstract Activated carbon paper-based materials were prepared from softwood pulp, activated carbon powder, and polyester fiber through wet forming process. Then polyethyleneimine was loaded on the activated carbon paper-based materials using physical impregnation method to fabricate green, low cost, and degradable PEI/activated carbon composite paper-based adsorbent materials (PPCA) for the removal of Cr(VI) from drinking water. The surface characteristics of the adsorbent were analyzed by SEM, EDX, BET, FT-IR, and XPS. It was found that the maximum adsorption capacity of Cr(VI) could reach up to 1.58 mg g^{-1} when the PEI immersion concentration is 1%, the contact time is 180 min, the temperature is 30 °C and pH$=2$. The adsorption of Cr(VI) on PPCA conformed to both the freundlich isotherm model and the quasi-second-order kinetic model, indicating that the adsorption was multi-molecular layer adsorption controlled by chemical reaction process. The adsorption mechanism of Cr(VI) on PPCA included electrostatic attraction, redox and chelation. Overall, this study provides a green, large-scalable production way for the preparation of biodegradable adsorption materials for the efficient removal of Cr(VI) from drinking water aiding the safe management of aqueous system.

T. Gao · C. Zhao (✉) · X. Li · Q. Ding (✉)
State Key Laboratory of Biobased Material and Green Papermaking, Qilu University of Technology, Shandong Academy of Sciences, Jinan 250353, China
e-mail: ppzcs78@163.com

Q. Ding
e-mail: xianshengding@qlu.edu.cn

T. Gao
e-mail: 531445992@qq.com

X. Li
e-mail: sqlixia126@126.com

S. Wang
Jiangsu Co-Innovation Center of Efficient Processing and Utilization of Forest Resources, Nanjing Forestry University, Nanjing 210037, China
e-mail: swang@njfu.edu.cn

Graphical abstract
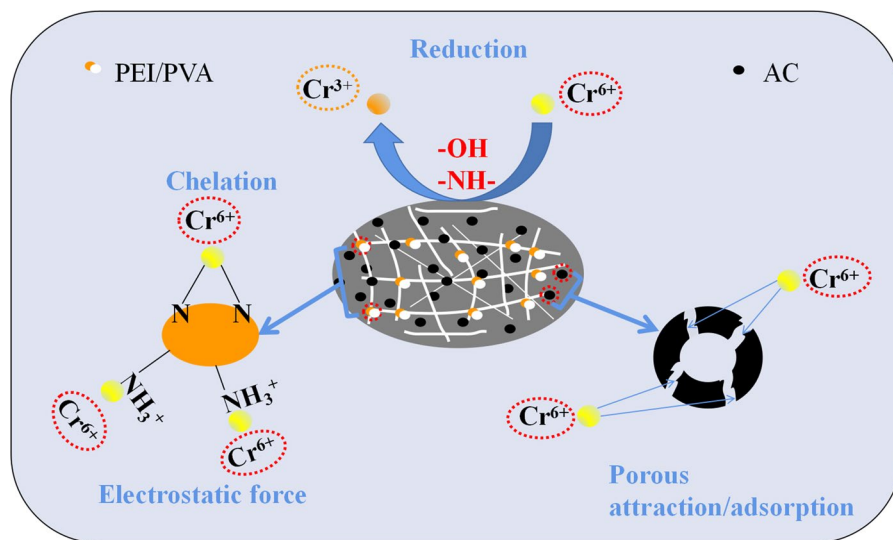
Introduction

In recent years, fast development continually along with industrialization and urbanization, industries the electronics industry, electroplating, petrochemical industry, leather tanning, and papermaking have brought benefits while also cause serious environmental contamination, especially chromium slags pollution (Ellis et al. 2002; Kobya et al. 2004). These chromium slags stored in open environment are not equipped with anti-seepage measures. Under the scouring of rainwater, they may seep into the ground, contaminate underground drinking water and eventually threaten human health (Fu et al. 2011). Chromium presences in two forms in water systems: Cr(III) and Cr(VI) (Guan et al. 2019). Cr(III) is one of the essential elements in animals (Huang et al. 2019). However, Cr(VI) is a highly toxic substance, which is easily absorbed by skin, causing the cancerization of human cells (Zhang et al. 2010; Lai et al. 2008) In China, the maximum allowable concentrations of Cr(VI) in industrial wastewater and drinking water are 0.5 mg L^{-1} and 0.05 mg L^{-1}, respectively.

The World Health Organization also requires that the Cr(VI) in drinking water should not exceed 0.05 mg L^{-1} (Demiral et al. 2008). Cr(VI) has been considered as one of the heavy metals to be removed preferentially. Therefore, it is urgent to develop green, low-cost adsorbents using a simple and large-scalable preparation method for the removal of Cr(VI) from drinking water (Chowdhury et al. 2016; Azimi et al. 2017).

The current methods for removing Cr(VI) from water commonly include membrane separation (Kozlowski et al. 2002), photochemical catalysis (Xu et al. 2019), ion exchange (Rengaraj et al. 2001), electrodialysis (Jin et al. 2016), and adsorption (Zhang et al. 2019; Sun et al. 2010) etc. In contrast, the adsorption method is commonly used to remove Cr(VI) from water due to its flexible utilization, and easy availability (Pang et al. 2011; Jin et al. 2017). A wide variety of adsorbents are available, including barks (Sudaryanto et al. 2021), chitosan (Zhang et al. 2021), cellulose nanocrystals (Tasrin et al. 2020), mesoporous silica (Li et al. 2021), activated carbon (Mojdeh et al. 2010), and synthetic hydrogel (Zhao et al. 2021), etc.

In the past few years, activated carbon had been widely used because of its large specific surface area and rich pore distribution (Sun et al. 2013). Activated carbon was used in fibrous, granular, or powder

form. Among them, activated carbon powder shows superior adsorption effect (Choi et al. 2008). However, activated carbon powder, if used alone may be dispersed in water, causing secondary pollution and increasing energy consumption for environmental pollution treatment. In the household water purifier, the activated carbon powder is compressed into a cake shape to reduce the loss of the activated carbon powder in water. However, the method is relatively cumbersome. To solve this problem, activated carbon powder was combined with softwood pulp to construct activated carbon paper-based materials.

Polyethyleneimine (PEI) is a high molecular polymer with abundant amino and imino groups, which can bind to heavy metals through chelation (Ma et al. 2014). PEI is a water-solublable. When it is directly used as an adsorbent, the adsorption ability decreases. Therefore, immobilizing PEI on activated carbon reduces its water solubility and improves its ability to remove heavy metals. Common fixation methods include physical impregnation and chemical grafting and cross-linking (Xing et al. 2021). Mojdeh Owlad (Mojdeh et al. 2010) immersed activated carbon in PEI water solution to prepare an absorbent to remove Cr(VI). When the initial concentration of Cr(VI) is 10 mg L^{-1}, its adsorption capacities reach 22 mg g^{-1} with a maximum removal rate of 80%. To further improve the loading rate of PEI, Pan (Pan et al. 2018) used glutaraldehyde as cross-linking agent to combine PEI with activated carbon by cross-linking method and explored the adsorption capacity to Cr(VI) in wastewater. It can be found that when the initial concentration of Cr(VI) is 350 mg L^{-1}, the removal rate is up to 98%, and the adsorption capacity is up to 500 mg g^{-1}. The adsorption effect is indeed significantly improved. However, its preparation conditions are harsh, the operation is cumbersome, and it is difficult to realize large-scale production and utilization. Glutaraldehyde is a toxic cross-linking agent, which is harmful when used in drinking water treatment. Therefore, it is particularly important to use non-toxic raw materials and simple processes to prepare adsorbents that can be used in drinking water purification. To the best of our knowledge, this is the first report on the use of PEI/activated carbon paper-based material (PPCA) fabricated by the combination of wet forming and physical impregnation method for the removal of low concentration of Cr(VI) from drinking water.

In this study, PPCA was prepared by wet forming process and impregnation methods, and various characterization methods were used to analyze their properties. The influence of pH, the concentration of PEI, contact time, temperature, adsorbent dosage, and the initial concentration of Cr(VI) on the Cr(VI) adsorption capacity in water were comprehensively explored. The adsorption mechanism of the PPCA to Cr(VI) was further discussed.

Experimental section

Materials

Softwood pulp was purchased from Dalian Yangrun Trading Co., Ltd. (Dalian, Liaoning). The polyester fiber was provided by Weifang Jiegao Fiber Co., Ltd. (Weifang, Shandong). Cationic polyacrylamide (CPAM) was purchased from Puyi Environmental Protection Technology Co., Ltd (Shanghai, China). Poly-amide epichlorohydrin resin (PAE) was purchased from Shandong Tongchuang Chemical Co., Ltd (Linyi Shandong). Activated carbon powder (200 mesh) was purchased from Lvzhiyuan, Pingdingshan City Original Activated Carbon Co., Ltd. (Pingding-shan, Henan). Potassium dichromate, diphenylcarbazide, polyethyleneimine (PEI), acetone, sulfuric acid, and polyvinyl alcohol (PVA) used in the experiment were all analytically pure and they were provided by Shanghai Aladdin Biochemical Technology Co., Ltd. (Shanghai, China). All chemicals were used as received without further purification.

Preparation of activated carbon paper-based materials

First of all, a certain amount of softwood pulp, polyester fiber, and activated carbon powder with a weight percentage of 42%, 10%, and 48%, respectively were weighted and dispersed in 1000 mL deionized water for 2000 r using a decomposing tank to form a stable suspension. Secondly, 0.08% CPAM and 0.8% PAE (weight of additive by weight of oven dry pulp) were added into the suspension mentioned above in the decomposing tank and then dispersed for another 2000 r to make sure their complete dissolution in water. Finally, The mixture was converted into a wet web using a hand sheet former (PK-3A, Austria PTI Co., Vienna, Austria). After a pressing stage, the wet

Fig. 1 Schematic of the synthesis of PPCA
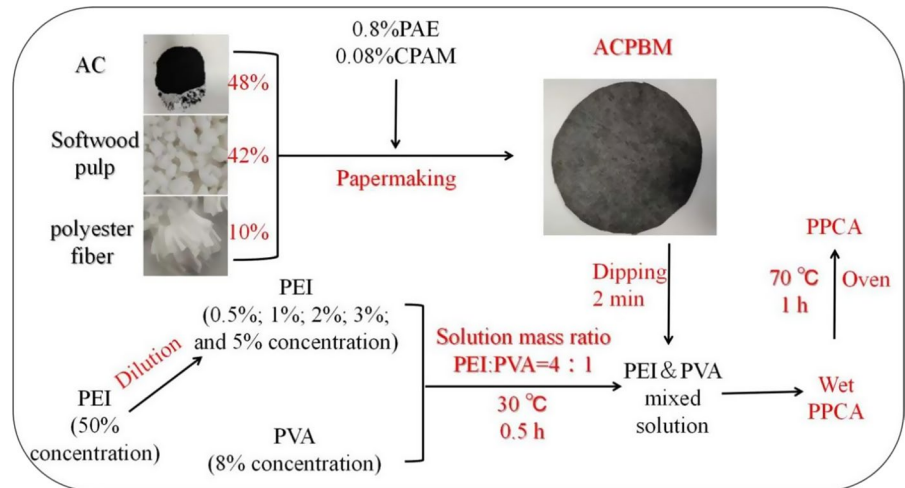
sheet was oven dried at 115 °C for 20 min to make activated carbon paper-based materials (ACPBM) (a basis weight of ACPBM of 240 g m^{-2}).

Preparation of PEI/PVA solution

First of all, 20 g of PVA was added into a beaker with 250 mL of deionized water and mechanically stirred for 1 h at 60 °C, followed by raising the temperature to 90 °C and continue stirring for another 2 h to prepare 8 wt.% PVA solution. Secondly, 0.5%, 1%, 2%, 3%, and 5% PEI solutions were prepared by diluting 50% PEI solution with a certain amount of deionized water. Finally, the desired amount of PVA and PEI solutions (a mass ratio of 1:4) were mixed and magnetically stirred in a water bath for 30 min at 30 °C to prepare PEI/PVA solutions with different concentrations.

Preparation of PPCA

Schematic of the synthesis of PPCA is shown in Fig. 1. Briefly, a desired amount of ACPBM was immersed in PEI/PVA mixture solutions with different concentrations for 2 min, and then taken out, followed by drying in a blast drying oven at 70 °C for 1 h. PPCA impregnated with 1% concentration of PEI was named as 1%PPCA.

Characterization of 1%PPCA

The surface morphology and size of 1%PPCA before and after the adsorption of Cr(VI) were characterized using scanning electron microscopy (SEM; Regulus 8220, Shimadzu Co., Tokyo, Japan). Energy dispersive X-ray spectroscopy (EDX) elemental mapping images obtained during SEM testing. The surface functional groups of samples were analyzed using an Fourier transform-infrared spectrometer (FT-IR; ALPHA, Bruker GmbH Co., Saarbrucken, Germany) in the range of 600–4000 cm^{-1}. The pore size distribution and specific surface area of the sample were evaluated using the N$_2$ adsorption and desorption isotherm obtained by BET (BELSORP MaxII, Maccheek Bayer Co., Tokyo, Japan) at 77 k. Zeta (z)-potential measurements were performed using a zetasizer (DTS1070-2, Malvern Instruments Co., Malvern, UK). Surface chemical compositions of 1%PPCA before and after water treatment were determined based on X-ray photoelectron spectroscopy (XPS; ESCALAB Xi+, Thermo Scientific Co., Massachusetts, US).

Adsorption experiments

First of all, a desired amount of adsorbent was added into a 250 mL conical flask with 100 mL of a certain concentration of Cr(VI) aqueous solution and then placed them in a vibrating screen with a preset temperature, followed by stirring at 170 rpm for different times. Subsequently, the above mentioned solutions

were taken out and filtered through a 0.45 μm filter membrane. The absorbance was measured at a wavelength of 540 nm using a three-purpose UV spectrophotometer in a dark box, and the Cr(VI) concentration was obtained according to Fig. S1.

The influence of concentrations of PEI solution (0.5, 1, 2, 3, and 5%), pH (2, 4, 6, 8, and 10), absorbent dosage (1, 3, and 5 g L^{-1}), initial Cr(VI) concentration (1, 5, 9, 12, and 15 mg L^{-1}), contact time (0.5, 1, 1.5, 2, 2.5, 3, 3.5, 4, 4.5, 5, 5.5, and 6 h), and temperature (20, 30, and 40 °C) on the Cr(VI) adsorption capacity were systematically investigated. All adsorption experiments were performed in triplicate and expressed as averages, with all errors < 3%. To study the adsorption mechanism of 1%PPCA, we fitted and analyzed the measured data by using adsorption kinetics, thermodynamics and isotherm.

Calculation of adsorption capacity and removal rate of Cr(VI)

The adsorption capacity and removal rate of PPCA on Cr(VI) are calculated according to formula (1) and formula (2) respectively:

$$Q = \frac{(C_0 = C_t)V}{m} \tag{1}$$

$$R = \frac{C_0 - C_t}{C_0} \tag{2}$$

where Q is the adsorption capacity of PPCA on Cr(VI) (mg g^{-1}); R is the removal rate of PPCA on Cr(VI) (%); C_0 is the initial concentration of Cr(VI) (mg L^{-1}); C_t is the concentration of Cr(VI) in the solution at time t (mg L^{-1}); V is the volume (L); M is the mass of PPCA (g).

Desorption studies

Cr(VI) anions were desorbed from 1%PPCA using NaOH aqueous solution (10 mL, 1 M). After shaking in a constant temperature water bath for 24 h, 2.5 mL of the desorbed solution was put into a 50 mL colorimetric tube and diluted to the mark by adding deionized water. Chromium ion concentration was calculated using the same method described in the

Fig. 2 SEM image of ACPBM (**a**); 1%PPCA (**b**); 1%PPCA after adsorption of Cr(VI) (**c**); and EDX elemental mapping images of the 1%PPCA after adsorption of Cr(VI) (**d–g**)
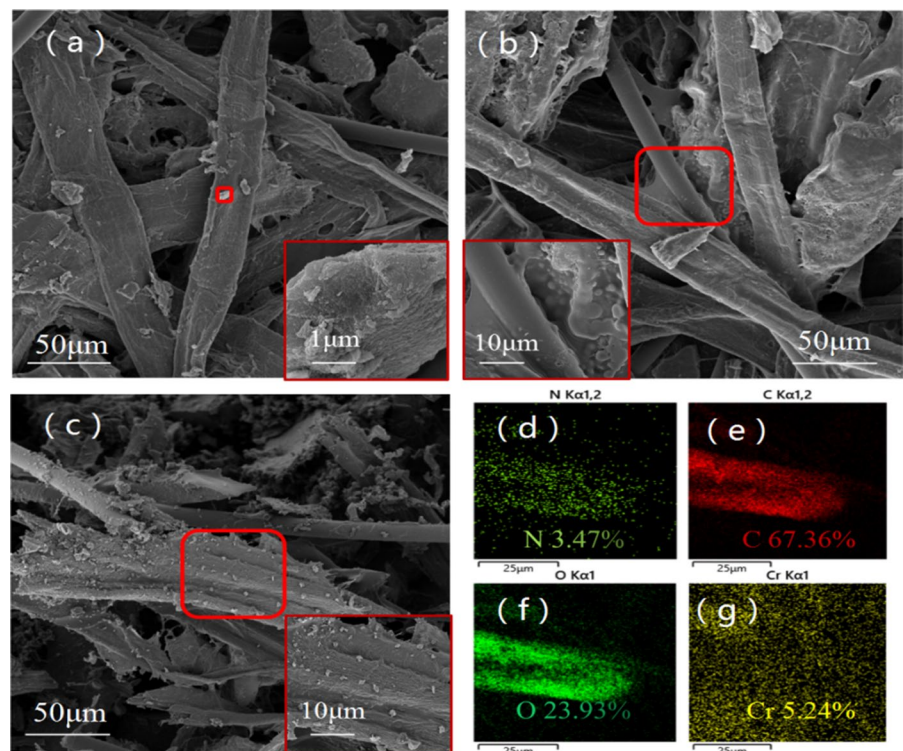
adsorption experimental section. After washing with 200 mL of deionized water and drying in a blast drying oven at 60 °C for 30 min, the 1%PPCA can be reused for the removal of Cr(VI) from water.

Results and discussion

Characterization

The surface morphology of ACPBM and 1%PPCA were observed by SEM (Fig. 2 and Fig. S4-S6). Softwood pulp fiber, one kind of plant fibers, is the main component of ACPBM. Because the surface of polyester fiber is relatively smooth, the interfacial binding force between polyester fiber and a plant fibers is weak, leading to the alternative arrangement of the polyester fiber and softwood pulp fiber in the sheet network. Activated carbon powder adheres to both the surface of polyester fibers and softwood pulp fibers (Fig. 2a). PEI/PVA solution can function as a glue-like substance between the fibers,thus giving rise to the reduction of pore size of the porous materials (Fig. 2b). Softwood pulp fibers swell due to water immersion, while polyester fibers are not affected (Fig. 2c). We also performed EDX analysis on the adsorbed material, it is found that the proportion of carbon, oxygen, nitrogen and chromium in the paper-based material is 67.36%, 23.93%, 3.47% and 5.24%, respectively. Chromium appeared in the 1%PPCA indicated that the paper-based material possessed a certain adsorption capacity on Cr(VI) (Fig. 2d, e).

The nitrogen adsorption capacity of the adsorbent increases with the increase of relative pressure (Fig. 3a). According to the classification of isotherms, it belongs to category VI isotherms. In the lower P/

Table 1 Pore structure characteristics of ACPBM, 1%PPCA and 2%PPCA

	Specific surface area (m^2 g^{-1})	Total pore volume (cm^3 g^{-1})
ACPBM	521.86	0.4088
1%PPCA	454.25	0.3322
2%PPCA	424.61	0.3103

P_0 zone, the capillary condensation of nitrogen occurs and agglomerates in the micropores on the inner surface area, which increases the adsorption capacity, giving rise to the rapidly rising of the isotherm, and a convex curve. With the increase of P/P_0, all pores have capillary aggregation, and adsorption only occurs on the outer surface, the specific surface area of which is much smaller than the inner surface, leading to the slow rising of the adsorption capacity. When the relative pressure is close to 1, nitrogen is adsorbed on the macropores, and the curve rises. In the range of P/P_0 of 0.43–1.0, the isotherm shows an obvious hysteresis loop. According to the classification of IUPAC, it belongs to the category VI mesoporous hysteresis ring, indicating that ACPBM is mainly composed of mesopores and micropores, and the pore structure is irregular. It is also found that as the concentration of impregnated PEI/PVA becomes larger, the adsorption capacity becomes smaller, which implies that PEI/PVA may adhere to the pores of activated carbon, resulting in a decrease in the specific surface area of the material (Table 1) and a decrease in the adsorption sites of nitrogen. Therefore, the adsorption capacity becomes smaller with increasing the concentration of PEI/PVA (Fig. 3a). The pores of ACPBM are mainly distributed in the range of 2–16 nm, and

Fig. 3 N$_2$ adsorption–desorption isotherms (**a**) and pore size distribution (**b**) of ACPBM, 1%PPCA and 2%PPCA
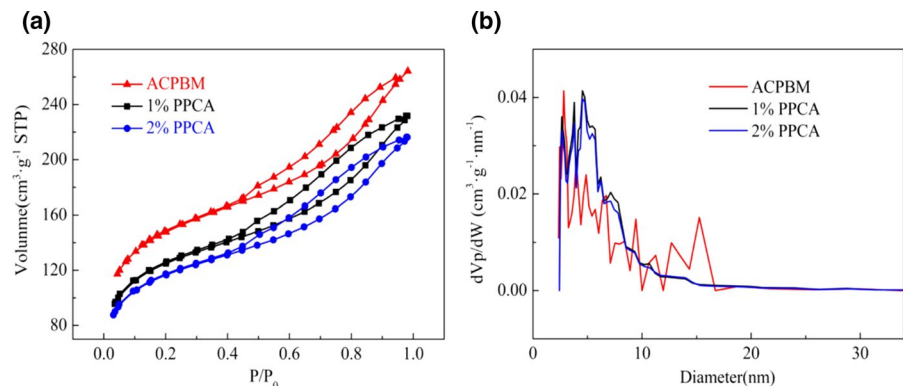
Fig. 4 FTIR spectra of ACPBM, 0.5%PPCA, 1%PPCA and 2%PPCA (**a**); Zeta-potential of 1%PPCA at various pH in deionized water (**b**)
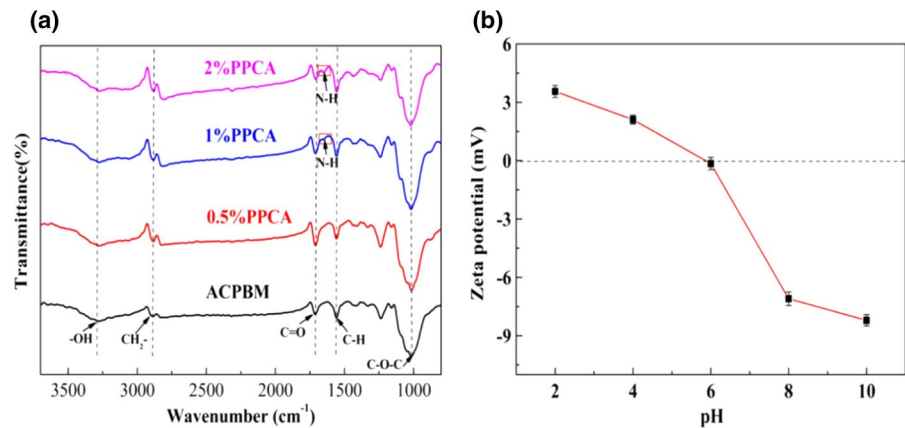
the pore size of 1%PPCA and 2%PPCA are mainly distributed in the range of 2–10 nm (Fig. 3b). This is mainly because the addition of PEI blocks the macropores.

The surface chemical structure of adsorbent impregnated with different concentrations of PEI/PVA solution were analyzed by infrared spectroscopy. The samples all showed typical characteristic absorption peaks of cellulose, such as -OH stretching vibration ($3270 \ cm^{-1}$), CH_2-stretching vibration ($2880 \ cm^{-1}$), C-H bending vibration ($1558 \ cm^{-1}$), and C–O–C stretching vibration ($1057 \ cm^{-1}$) (Shao et al. 2021). The characteristic absorption peaks at $1705 \ cm^{-1}$ are the C=O stretching vibrations in the polyester fiber (Ricardo et al. 2015) (Fig. 4a). It was also find that as the concentration of the coated PEI increases, there is an obvious small peak near $1650 \ cm^{-1}$, which is the result of the N–H bending vibration of PEI. In addition, PEI should have N–H stretching vibration peaks and C-N stretching vibration peaks at $3270 \ cm^{-1}$ and $1045 \ cm^{-1}$ (Hong et al. 2021). However, ACPBM, 0.5%PPCA, 1%PPCA, and 2%PPCA all have characteristic peaks at these two wavelengths. The N–H and the C-N stretching vibration peak in the PEI are covered by the O–H and the C–O–C stretching vibration peak in the cellulose, respectively (Fig. 4a). The above analysis shows that PEI has been successfully loaded onto the ACPBM.

Effects of PEI solution concentration

The removal rate and the adsorption capacity of Cr(VI) by ACPBM is 90.15%, of $1.50 \ mg \ g^{-1}$,

respectively. Both of them increase with the impregnated PEI concentration. When the impregnated PEI concentration is 1%, the adsorption capacity and removal rate of Cr(VI) reaches the maximum value of $1.58 \ mg \ g^{-1}$ and 94.88%, respectively (Fig. 5a). This is mainly because not only the activated carbon has an adsorption effect on Cr(VI), but also the amino groups in PEI can remove Cr(VI) through chelation. As the concentration of impregnation increases, the amino groups in the adsorbent increase, endowing the adsorbent with better adsorption ability. However, with the concentration of impregnation further increases, the adsorption ability of adsorbent on Cr(VI) decreases (Fig. 5a). This can be explained by that a large amount of PEI adheres to the surface of the activated carbon results in a decrease in the specific surface area (Table 1) of the activated carbon and a decrease in the adsorption sites for Cr(VI).

Effects of initial pH

Cr(VI) in aqueous solution mainly exists in three forms: $Cr_2O_7^{2-}$, CrO_4^{2-}, and $HCrO_4^{-}$, and the mutual conversion between them is affected by pH (Pan et al. 2018). Under acidic conditions, Cr(VI) in the solution mainly exists in the form of $Cr_2O_7^{2-}$ and $HCrO_4^{-}$. With the increase of pH, the content of hydrogen ions decreases, and the conversion proceeds in the direction of generating $HCrO_4^{-}$. Under alkaline conditions or neutral conditions, Cr(VI) mainly exists in the form of CrO_4^{2-} (Sun et al. 2013; Ma et al. 2014).
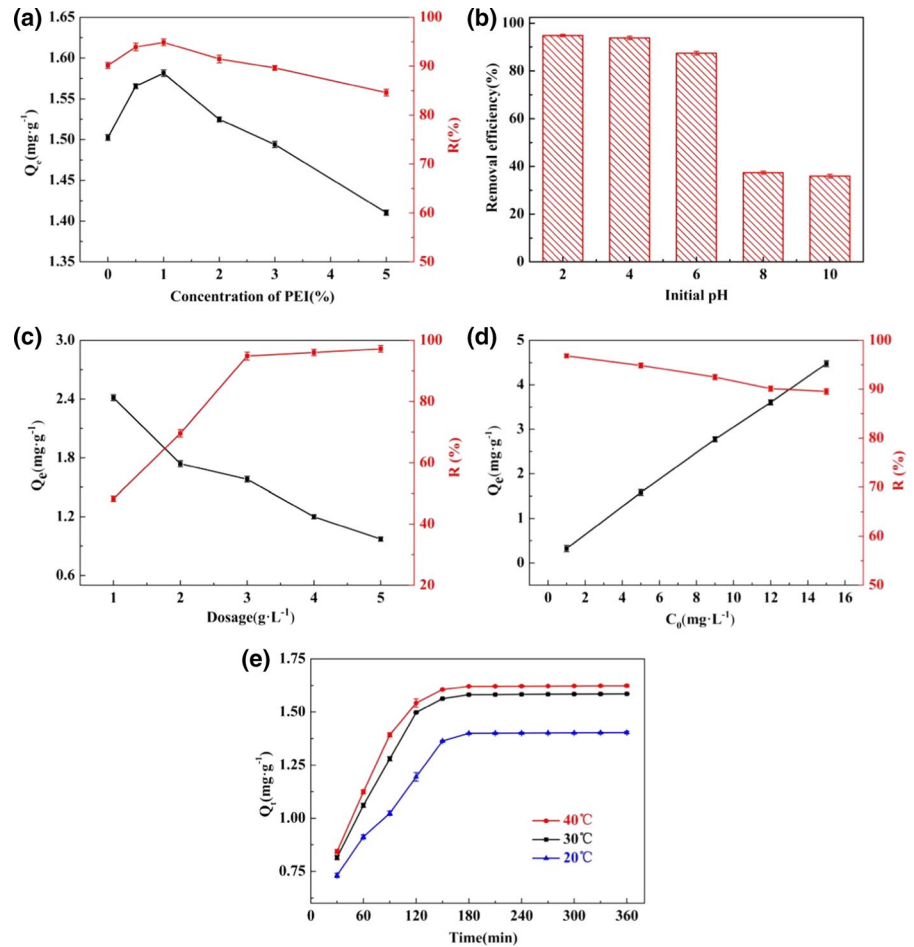
PEI is a positively charged polymer, and the protonation of surface amino groups is the main factor that affects the cationic charge density of PEI. The stronger the protonation ability of the amino groups on the PEI surface, the greater the cationic charge density on the surface. It has a strong adsorption effect on the anions existing in the solution.

The removal rate of Cr(VI) by 1%PPCA reaches the maximum value of 94.88% at pH of 2. As the pH value increases, the removal rate gradually decreases (Fig. 5b). This is mainly because (1) in the acidic solution of pH = 2, the hydrogen ion content in the solution is higher, which makes the amino group in PEI easier to protonate. Therefore, the $HCrO_4^-$ and $Cr_2O_7^{2-}$ existing in the form of anions in the solution can be better electrostatically adsorbed; (2) the electrostatic repulsion between the 1%PPCA surface and Cr(VI) anions hindered the removal ability of Cr(VI) under high pH conditions

(Zhao et al. 2015); (3) the redox potential of Cr(VI)/Cr(III) at low pH values was significantly higher than that at high pH values.

From the Zeta potential, we can be seen that when pH = 6, the charge in the solution is 0, showing electrical neutrality. When pH < 6, the solution is positively charged (Fig. 4b). With the decrease of pH, the binding ability of positively charged nitrogen (N^+) on the surface of PEI to Cr(VI) in the form of anion is stronger, and the adsorption effect will be better. Therefore, when pH = 2, 1%PPCA has the best adsorption effect on Cr(VI).

Effects of dosage

Wirh the dosage of 1%PPCA increased from 1 g L^{-1} to 3 g L^{-1}, the removal rate of Cr(VI) increased significantly, from 44.44% to 94.45% (Fig. 5c). The main reason is that when the dosage of 1%PPCA is

small, the adsorption sites of Cr(VI) are few. With the increase of the dosage of 1%PPCA, the adsorption sites for Cr(VI) increases, which significantly improves the adsorption effect. Continuing to increase the dosage of 1%PPCA, the Cr(VI) removal rate exhibits a saturation plateau (Fig. 5c). This is mainly because the adsorption of Cr(VI) in water by 1%PPCA has reached adsorption equilibrium. Even if the dosage is increased, the removal rate of Cr(VI) will not be significantly improved. However, the adsorption capacity of Cr(VI) decreases with the increase of the dosage of 1%PPCA, which is mainly because: (1) when the adsorption site exceeds the adsorption site required for saturation, the adsorption capacity decreases; (2) when calculating the adsorption capacity with formula (1), the dosage is used as the denominator, and its value has a great impact on the adsorption capacity. The larger the value, the smaller the adsorption capacity (Fig. 5c).

Effects of initial concentration of Cr(VI)

The adsorption capacity of Cr(VI) increases with the increase of the initial concentration of Cr(VI), from 0.2 mg g^{-1} to 4.96 mg g^{-1} (Fig. 5d). This is mainly because that as the initial concentration of Cr(VI) increases, the difference between the concentration of Cr(VI) in water and the concentration of 1%PPCA surface becomes larger, so the adsorption performance is enhanced and the adsorption capacity is increased. The removal rate of Cr(VI) decreases with the increase of the initial concentration of Cr(VI) (Fig. 5d). This can be explained by that as the initial concentration of Cr(VI) increases, the capacity of Cr(VI) that needs to be adsorbed in water increases, however, the adsorption capacity of 1%PPCA is constant. When the adsorption sites on the surface of 1%PPCA are all occupied, Cr(VI) is no longer adsorbed by 1%PPCA.

Effects of time and temperature

As the adsorption contact time increases, the adsorption capacity also increases. When the contact time is 180 min, the adsorption capacity reaches the maximum value of 1.58 mg g^{-1} (Fig. 5e). When the contact time further increases from 180 to 360 min, the adsorption capacity is unchanged, which

indicates that the adsorption has reached the adsorption equilibrium.

The capacity of adsorption increases with the increase of temperature, which shows that temperature rise is conducive to the adsorption of Cr(VI) from water. When the temperature increased from 20 to 30 °C, the adsorption capacity increases significantly from 1.37 mg g^{-1} to 1.53 mg g^{-1}. When further increasing the temperature from 30 to 40 °C, the adsorption capacity increases slowly (Fig. 5e). This may be because the increase of temperature can accelerate the diffusion rate and improve the adsorption performance of 1%PPCA for Cr(VI). However, when the temperature is too high, the material may be easily damaged, so the adsorption effect increases slowly. Thus, the optimal adsorption temperature is 30 °C.

Adsorption kinetics

Adsorption kinetics is mainly used to describe the adsorption rate of the adsorbent. There are three adsorption kinetic models, namely the quasi-first-order, the quasi-second-order adsorption kinetic equation, and the intra-particle diffusion model (Xiao et al. 2017). Fitting the adsorption data with these three equations can reveal the adsorption mechanism of the adsorbent.

The quasi-first-order adsorption kinetic equation is the proportional relationship between the reaction adsorption rate and the concentration of reactants, and its linear expression (Indra et al. 2005) is:

$$\log \left(Q_e - Q_t \right) - k_1 t + \log Q_e \tag{3}$$

where Q_e is the equilibrium adsorption capacity (mg g^{-1}), Q_t is the adsorption capacity at time t (mg g^{-1}), and k_1 is the reaction rate constant of the quasi-first order adsorption kinetic equation.

The quasi-second-order kinetic equation assumes that the adsorbent and the adsorbate undergo a chemical reaction, and the adsorption rate is affected by the chemical adsorption process. This process involves the gains and losses of electrons or the sharing of electrons. Its linear expression (Indra et al. 2005) is:

$$\frac{t}{Q_t} = \frac{t}{Q_e} + \frac{1}{k_2 Q_e} \tag{4}$$

where k_2 is the adsorption rate constant of the quasi-second-order kinetic equation, $h = k_2 Q_e$ is the initial adsorption rate constant (mg g^{-1} h^{-1}).

The intra-particle diffusion model is mainly used to describe the process of adsorbent diffusion to the surface of the adsorbent through macropores or micropores. Its linear expression (Indra et al. 2005) is:

$$Q_t = k_3 t^{\frac{1}{2}} + Q_e \tag{5}$$

where k_3 is the diffusion rate constant within the particle (mg g^{-1} h$^{-0.5}$), the larger the value, the easier the adsorbate diffuses inside the adsorbent.

The quasi-second-stage adsorption kinetic equation not only has a high degree of fit, but also its Q_e is closer to $q_{e.\ Exp}$ (Fig. S2a-b and Table S2). This shows that this process is controlled by chemical reactions. We can also find the process of 1%PPCA adsorption of Cr(VI) can be divided into two stages. The $R^2 > 0.99$ of the two stages indicates that Q_t has a linear relationship with $t^{0.5}$, and there is intra-particle diffusion in this process. The k_3 of the first stage is 0.87659, and the k_3 of the second stage is 0.00525 (Fig. S2c and Table S2). It shows that the adsorbent in the first stage is prone to internal diffusion in the adsorbate. This is mainly because there is a large concentration difference between the 1%PPAC surface and the Cr(VI) at the beginning of the reaction, and the mass transfer driving force is large. Particles are mainly diffused through macropores, so particle diffusion is easy with. As the reaction proceeds, the adsorption sites on the surface of 1%PPCA are gradually occupied by chromium ions, which reduces the adsorption rate. At this time, the particles diffuse mainly through the micropores inside the adsorbate.

Adsorption isotherm

The adsorption isotherm expresses the relationship between adsorption capacity and solution concentration when adsorption reaches equilibrium at a certain temperature. It can describe the mechanism of action between adsorbate and adsorbent, which has a great effect in exploring the surface characteristics of adsorbate and adsorbent (Guo et al. 2017a, 2017b).

The langmuir isotherm is used to show that the adsorption reaction is a monolayer surface adsorption.

Many uniform adsorption active sites are distributed on the adsorbent, and one molecule can only be adsorbed to one active site (Charpentier et al. 2016). When the surface adsorption active sites are all occupied, the adsorption capacity reaches the saturation value. The equation (Indra et al. 2005) is:

$$\frac{1}{Q_e} = \frac{1}{Q_0} + \frac{1}{b Q_e C_e} \tag{6}$$

Convert it into a linear expression (Indra et al. 2005) as:

$$\frac{C_e}{Q_e} = \frac{1}{bQ} + \frac{C_e}{Q_0} \tag{7}$$

where C_e is the equilibrium concentration (mg L^{-1}); Q_0 is the maximum adsorption capacity for single-molecule adsorption (mg g^{-1}); b is the Langmuir constant, which indicates the binding force between the adsorbent and the adsorbate.

The freundlich isotherm indicates that the adsorption reaction belongs to multi-molecular layer adsorption (Lin et al. 2017a, 2017b). The active adsorption sites are unevenly distributed on the adsorbent. The equation (Indra et al. 2005) is:

$$\lg Q_e = \lg K_F + \frac{\lg C_e}{n} \tag{8}$$

where K_F is the equilibrium adsorption constant, which reflects the strength of the adsorption capacity; 1/n is the composition factor, which indicates the strength of the adsorption capacity increases with the concentration, and reflects the difficulty of adsorption.

The Freundlich adsorption isotherm better reflects the adsorption behavior of 1%PPCA for Cr(VI), indicating that the adsorption of 1%PPCA on Cr(VI) is multi-molecular layer adsorption. It can be seen from the table S2 that $n > 1$, indicating that the adsorption reaction is easy to proceed. The maximum adsorption capacity of 1%PPCA for Cr(VI) is 6.62 mg g^{-1} (Fig. S3a-b and Table S2).

Adsorption thermodynamics

To explain the effect of temperature on the adsorption of chromium ions, it is very important to calculate the thermodynamic constants of adsorption. The

thermodynamic isotherm is mainly used to evaluate the change of energy and entropy of the adsorbent during the adsorption process. The equation between the Gibbs free energy change (ΔG_0) and the distribution coefficient K_D (Indra et al. 2005) is:

$$\Delta G_0 = -RT\text{In}K_D \qquad (9)$$

The equations of enthalpy change (ΔH_0), entropy change (ΔS_0) and ΔG_0 (Indra et al. 2005) are as follows:

$$\Delta G_0 = \Delta H_0 - T\Delta S_0 \qquad (10)$$

Combining this formula (9) with formula (10), the Vanter Hoff equation (Indra et al. 2005) is obtained as follows:

$$In\ K_D = -\frac{\Delta G_0}{RT} = \frac{\Delta S_0}{R} - \frac{\Delta H_0}{RT} \qquad (11)$$

where R is the gas constant 0.008314 kJ mol^{-1} K^{-1}; T is the absolute temperature K.

It can be seen from Fig. S3c and Table S3 that $\Delta H_0 > 0$ in the adsorption process of Cr(VI) by 1%PPCA, indicating that the reaction is an endothermic reaction. Thus, the adsorption performance improved gradually with the increase of temperature. $\Delta S_0 > 0$, indicates the entropy increases during the adsorption process of Cr(VI) by 1%PPCA, which means that the complexity and stability of adsorption, and the degree of freedom of the liquid–solid surface increase. From table S3, we can also find that $\Delta G_0 < 0$, indicating that this reaction can proceed spontaneously. As the temperature increases, ΔG_0 gradually becomes smaller, which further shows that increasing the temperature can promote the adsorption progress.

Adsorption mechanism of Cr(VI) by 1%PPCA

XPS was used to analyze the chemical elemental composition of the surface before and after the adsorption of chromium ions by 1%PPCA. The 1%PPCA before adsorption has obvious energy bands at 531.9, 397.9 and 284.3 eV, and these peaks are assigned to O1 s, N1 s and C1s, respectively

Fig. 6 XPS characterization of 1%PPCA before (**a**) and after(**b**) Cr(VI) adsorption, Cr 2p high resolution spectra (**c**)
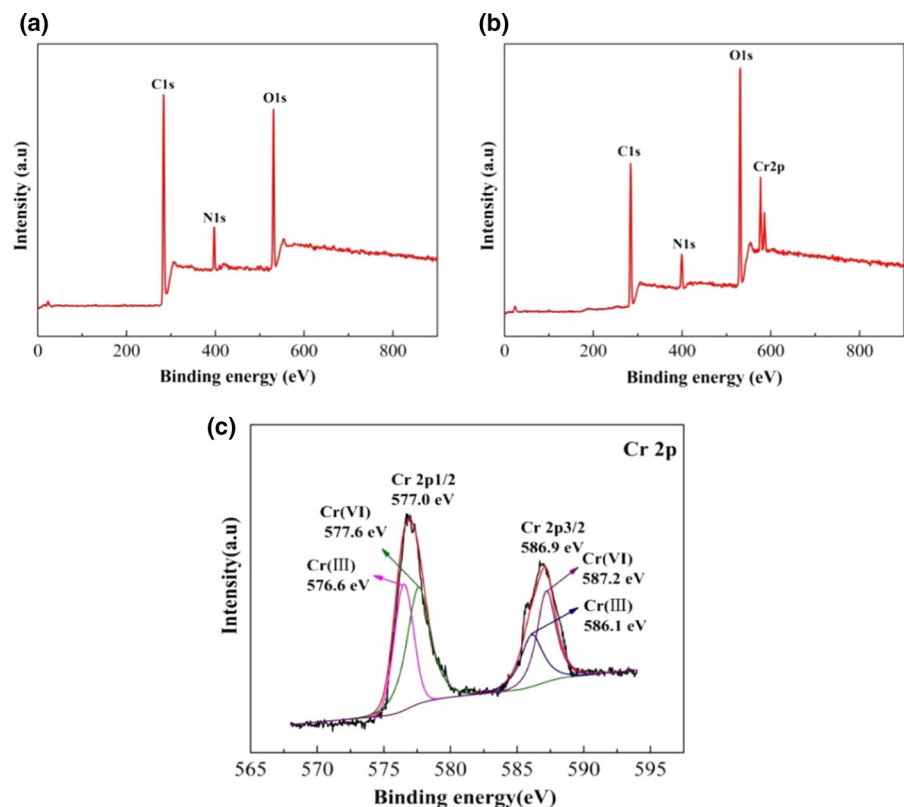
Fig. 7 The mechanism of 1%PPCA for the removal of Cr(VI)
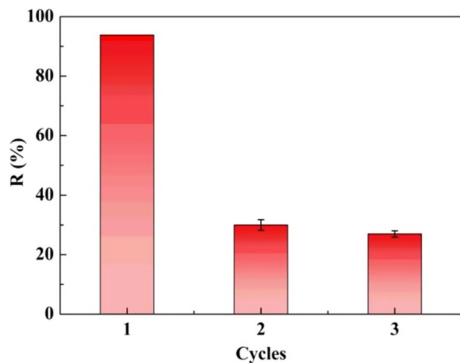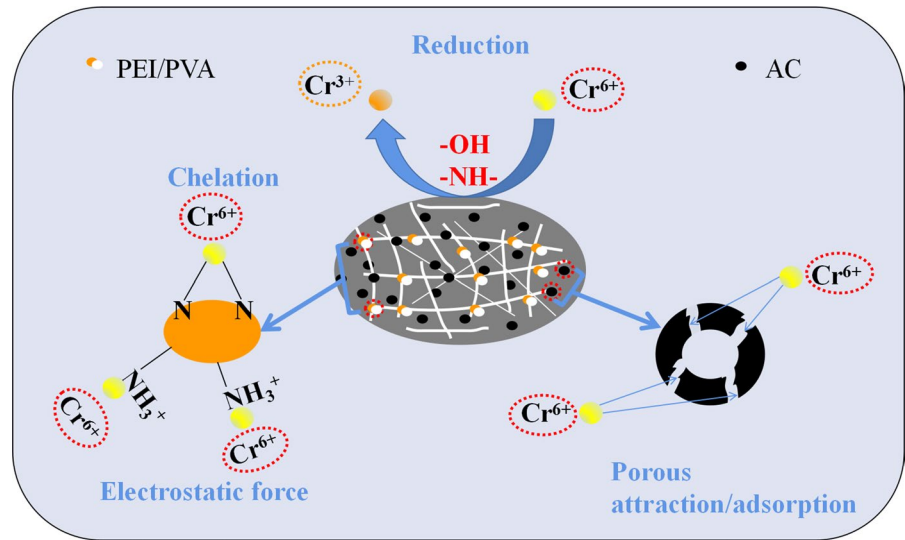
Fig. 8 Adsorption/desorption cycles of 1%PPCA in Cr(VI) adsorption after third recycle

(Wan et al. 2017). Compared with 1%PPCA before adsorption, two new energy bands appeared at 586.8 eV and 577.3 eV for 1%PPCA after adsorption, which were assigned to Cr2p1/2 and Cr2p3/2, respectively (Fig. 6a-b) (Ballav et al. 2012; Zhang et al. 2016). The adsorbed 1%PPCA contained Cr2p1/2 and Cr2p3/2, which also indicated that Cr(VI) and Cr(III) coexisted on the surface of the material. In addition, the energy of O1 s showed an obvious upward trend, while the energy of N1 s and C1s decreased, which may be due to the reaction of chromium ions with the amino and C elements in the material. The adsorption mechanism was further studied, and the spectra of Cr2p3/2 and Cr2p1/2 could be divided into two peaks (Fig. 6c). One is

Cr(III) centered at 576.6 eV and 586.1 eV; the other is Cr(VI) centered at 577.6 eV and 587.2 eV. This may be due to the presence of abundant hydroxyl and amino groups on the surface of the material, which can act as electron donors for the reduction of Cr(VI) (Chen et al. 2018). The result is also confirmed by previously reported studies (Zhao et al. 2015; Fang et al. 2018; Shao et al. 2021).

In summary, the adsorption mechanism of Cr(VI) by 1%PPCA (Fig. 7) in this experiment mainly includes the following aspects: (1) Cr(VI) can be adsorbed on the porous activated carbon surface; (2) Cr(VI) is reduced to Cr(III) by a large number of hydroxyl and amino groups on the surface of the material; (3) N–N in the material can be combined with Cr(VI) through chelation, thereby being removed; (4) Electrostatic attraction is formed between NH_3^+ in polyethyleneimine and Cr(VI).

Desorption studies

Dilute NaOH solution (1 M) was used to desorb Cr(VI) from the 1%PPCA Surface while prevent the degradation of the adsorbent. The mechanism of desorption may be the replacement of chromate anions (Mallampati et al. 2013) and protonated cations (Wan et al. 2008) with hydroxyl ions. The adsorption effect of the desorbed material on Cr(VI) showed a significant downward trend (Fig. 8). This may be because PEI has a strong binding ability to Cr(VI) through chelation, and has a low desorption

efficiency, resulting in a decrease in the adsorption performance of the desorbed material. This study also demonstrated that the material is disposable.

This material is mainly composed of plant fibers and activated carbon. Plant fibers are easily degraded in soil. Activated carbon has a poorer degradability than plant fibers, but it is a non-toxic material and has less environmental pollution. All in all, a green, low-cost, disposable paper-based adsorption material was successfully prepared for the efficient removal of chromium ions from drinking water. The fabrication method is straightforward and large-scalable, providing a new way for the design of other biomass-based adsorption materials.

Conclusions

In this study, a green, low cost, and degradable disposable adsorption material was prepared by a combination of wet forming process and physical impregnation method. The adsorption effect of the 1%PPCA was greatly affected by the pH, and the optimal pH was 2, and the adsorption capacity could reach 1.58 mg g^{-1}. The adsorption process of Cr(VI) by 1%PPCA for was multi-molecular layer adsorption and the adsorption was controlled by chemical reactions. The process of adsorbing Cr(VI) by the 1%PPCA could proceed spontaneously. The adsorption mechanism of Cr(VI) on 1%PPCA included electrostatic attraction, redox and chelation. Even though this material shows inferior adsorption capacity when compared with other heavy metal adsorbents, but it has the advantages of degradability, low-cost and and scalable production. All in all, the developed green PPCA adsorption materials had a certain removal effect on low-concentration Cr(VI), and was expected toused as the outermost layer of domestic water purifier to remove particulate matter, residual chlorine, heavy metals and other pollutants from drinking water.

Author contributions Material preparation, data collection and analysis were performed by [Tianliang Gao]. The first draft of the manuscript was written by [Tianliang Gao] and all authors commented on previous versions of the manuscript. All authors read and approved the final manuscript.

Declarations

Conflict of interest The authors have no relevant financial or non-financial interests to disclose.

References

Azimi A, Azari A, Rezakazemi M, Ansarpour M (2017) Removal of heavy metals from industrial wastewaters: a review. ChemBioEng Rev 4:37–59. https://doi.org/10.1002/cben.201600010

Ballav N, Maity A, Mishra SB (2012) High efficient removal of chromium(VI) using glycine doped polypyrrole adsorbent from aqueous solution. Chem Eng J 198–199:536–546. https://doi.org/10.1016/j.cej.2012.05.110

Charpentier TVJ, Neville A, Lanigan JL, Barker RJ, Richardson T (2016) Preparation of magnetic carboxymethylchitosan nanoparticles for adsorption of heavy metal ions. ACS Omega 1:77–83. https://doi.org/10.1021/acsomega.6b00035

Chen SX, Wang J, Wu ZL, Deng Q, Tu WF, Dai GP, Zeng ZL, Deng SG (2018) Enhanced Cr(VI) removal by polyethylenimine- and phosphorus-codoped hierarchical porous carbons. J Colloid Sci 523:110–120. https://doi.org/10.1016/j.jcis.2018.03.057

Choi KJ, Kim SG, Kim SH (2008) Removal of tetracycline and sulfonamide classes of the antibiotic compound by powdered activated carbon. Environ Technol 29:333–342. https://doi.org/10.1080/09593330802102223

Chowdhury S, Mazumder MJ, Al-Attas O, Husain T (2016) Heavy metals in drinking water: occurrences, implications, and future needs in developing countries. Sci Total Environ 569–570:476–488. https://doi.org/10.1016/j.scitotenv.2016.06.166

Demiral H, Demiral I, Tumsek F, Karabacakoglu B (2008) Adsorption of chromium(VI) from aqueous solution by activated carbon derived from olive bagasse and applicability of different adsorption models. Chem Eng J 144:188–196. https://doi.org/10.1016/j.cej.2008.01.020

Ellis AS, Johnson TM, Bullen TD (2002) Chromium isotopes and the fate of hexavalent chromium in the environment. Sci 295:2060–2062. https://doi.org/10.1126/science.1068368

Fang W, Jiang X, Luo H, Geng J (2018) Synthesis of graphene/SiO$_2$@ polypyrrole nanocomposites and their application for Cr(VI) removal in aqueous solution. Chemosphere 197:594–602. https://doi.org/10.1016/j.chemosphere.2017.12.163

Fu F, Wang Q (2011) Removal of heavy metal ions from wastewaters: a review. J Environ Manage 92:407–418. https://doi.org/10.1016/j.jenvman.2010.11.011

Guan X, Yang H, Sun Y, Qiao J (2019) Enhanced immobilization of chromium(VI) in soil using sulfidated zero-valent

iron. Chemosphere 228:370–376. https://doi.org/10.1016/j.chemosphere.2019.04.132

Guo DM, An QD, Xiao ZY, Zhai SR, Shi Z (2017a) Polyethylenimine-functionalized cellulose aerogel beads for efficient dynamic removal of chromium(vi) from aqueous solution. RCS Adv 7:54039–54052. https://doi.org/10.1039/c7ra09940a

Guo XZ, Ding L, Kanamori K, Nakanishi K, Yang H (2017b) Functionalization of hierarchically porous silica monoliths with polyethyleneimine(PEI) for CO_2 adsorption. Microporous Mesoporous Mater 254:51–57. https://doi.org/10.1016/j.micromeso.2017.02.076

Hong HJ, Ban G, Kim HS, Jeong HS, Park MS (2021) Fabrication of cylindrical 3D cellulose nanofibril (CNF) aerogel for continuous removal of copper(Cu^{2+}) from wastewater. Chemosphere 278:130288. https://doi.org/10.1016/J.CHEMOSPHERE.2021.130288

Huang D, Liu C, Zhang C, Deng R, Wang R, Xue W, Luo H, Zeng G, Zhang Q, Guo X (2019) Cr(VI) removal from aqueous solution using biochar modified with Mg/Al-layered double hydroxide intercalated with ethylene-diamine-tetraacetic acid. Bioresour Technol 276:127–132. https://doi.org/10.1016/j.biortech.2018.12.114

Indra DM, Vimal CS, Nitin KA, Indra MM (2005) Removal of congo red from aqueous solution by bagasse fly ash and activated carbon: kinetic study and equilibrium isotherm analyses. Chemosphere 61:492–501. https://doi.org/10.1016/j.chemosphere.2005.03.065

Jin W, Du H, Zheng S, Zhang Y (2016) Electrochemical processes for the environmental remediation of toxic Cr(VI): a review. Electrochim Acta 191:1044–1055. https://doi.org/10.1016/j.electacta.2016.01.130

Jin X, Xiang Z, Liu Q, Chen Y, Lu F (2017) Polyethyleneimine-bacterial cellulose biosorbent for effective removal of copper and lead ions from aqueous solution. Bioresour Technol 244:844–849. https://doi.org/10.1016/j.biortech.2017.08.072

Kobya M (2004) Removal of Cr(VI) from aqueous solutions by adsorption onto hazelnut shell activated carbon: kinetic and equilibrium Studies. Bioresour Technol 91:317–321. https://doi.org/10.1016/j.biortech.2003.07.001

Kozlowski CA, Walkowiak W (2002) Removal of chromium(vi) from aqueous solutions by polymer inclusion membranes. Water Res 36:4870–4876. https://doi.org/10.1016/S0043-1354(02)00216-6

Lai KCK, Lo IC (2008) Removal of chromium (VI) by acid-washed zero-valent iron under various groundwater geochemistry conditions. Environ Sci Technol 42:1238–1244. https://doi.org/10.1021/es071572n

Li SL, Li SQ, Wen N, Wei D, Zhang YF (2021) Highly effective removal of lead and cadmium ions from wastewater by bifunctional magnetic mesoporous silica. Sep Purif Technol 265:118341–118352. https://doi.org/10.1016/J.SEPPUR.2021.118341

Lin F, You Y, Yang X, Jiang X, Lu B (2017a) Microwave-assisted facile synthesis of TEMPO-oxidized cellulose beads with high adsorption capacity for organic dyes. Cellulose 24:5025–5040. https://doi.org/10.1007/s10570-017-1473-9

Lin Y, Hong Y, Song Q, Zhang Z, Gao J, Tao T (2017b) Highly efficient removal of copper ions from water

using poly(acrylic acid)-grafted chitosan adsorbent. Colloid Polym Sci 295:627–635. https://doi.org/10.1007/s00396-017-4042-8

Ma Y, Liu WJ, Zhang N, Li YS, Jiang H, Sheng GP (2014) Polyethylenimine modified biochar adsorbent for hexavalent chromium removal from the aqueous solution. Bioresour Technol 169:403–408. https://doi.org/10.1016/j.biortech.2014.07.014

Mallampati R, Valiyaveettil S (2013) Apple peels-a versatile biomass for water purification? ACS Appl Mater Interfaces 5:4443–4449. https://doi.org/10.1021/am400901e

Mojdeh O, Mohamed KA, Wan MAWD (2010) Hexavalent chromium adsorption on impregnated palm shell activated carbon with polyethyleneimine. Bioresour Technol 101:5098–5103. https://doi.org/10.1016/j.biortech.2010.01.135

Pan RR, Zou JX, Li Y, Jin XJ (2018) Hyperbranched polyethylenimine modified waste fiberboard activated carbon for enhanced adsorption of hexavalent chromium. J Wood Chem Technol 3813:1–12. https://doi.org/10.1080/02773813.2017.1388820

Pang Y, Zeng GM, Tang L, Zhang Y, Liu YY, Lei XX, Li Z, Zhang JC, Xie GX (2011) PEI-grafted magnetic porous powder for highly effective adsorption of heavy metal ions. Desalination 28:278–284. https://doi.org/10.1016/j.desal.2011.08.001

Rengaraj S, Yeon KH, Moon SH (2001) Removal of chromium from water and wastewater by ion exchange resins. J Hazard Mater 87:273–287. https://doi.org/10.1016/S0304-3894(01)00291-6

Ricardo M, Edwin AM (2015) Hyperbranched polyester polyol modified with polylactic acid. J App Polym Sci 132:41589. https://doi.org/10.1002/app.41589

Shao YT, Fan ZH, Zhong MF, Xu W, He C, Zhang ZJ (2021) Polypyrrole/bacterial cellulose nanofiber composites for hexavalent chromium removal. Cellulose 28:2229–2240. https://doi.org/10.1007/S10570-020-03660-2

Sudaryanto Y, Anggorowati AA, Sianto ME (2021) Study of Pb (II) adsorption by tannin based adsorbent from mangrove bark (Rhizophora mucronate). J Phys: Conf Ser 1858:012083–101289. https://doi.org/10.1088/1742-6596/1858/1/012086

Sun XF, Ma Y, Liu XW, Wang SG, Gao BY, Li XM (2010) Sorption and detoxifii-cation of chromium(VI) by aerobic granules functionalized with polyethylenimine. Water Res 44:2517–2524. https://doi.org/10.1016/j.watres.2010.01.027

Sun YY, Yue QY, Gao BY, Gao Y, Li Q, Wang Y (2013) Adsorption of hexavalent chromium on arundodonax linn activated carbon amine-crosslinked copolymer. Chem Eng J 217:240–247. https://doi.org/10.1016/j.cej.2012.11.121

Tasrin S, Mohamed MFS, Padmanaban VC, Selvaraju N (2020) Surface modification of nanocellulose using polypyrrole for the adsorptive removal of Congo red dye and chromium in binary mixture. Int J of Biol Macromol 151:322–332. https://doi.org/10.1016/j.ijbiomac.2020.02.181

Vedenyapina MD, Kurmysheva AY, Kulaishin SA, Kryazhev YG (2021) Adsorption of heavy metals on activated carbons (a Review). Solid Fuel Chem 55:83–104. https://doi.org/10.3103/S0361521921020099

Wan NWS, Hanafiah MAKM (2008) Removal of heavy metal ions from wastewater by chemically modified plant wastes as adsorbents: a review. Bioresour Technol 99:3935–3948. https://doi.org/10.1016/j.biortech.2007.06.011

Wan C, Jiao Y, Li J (2017) Flexible, highly conductive, and free-standing reduced graphene oxide/polypyrrole/cellulose hybrid papers for supercapacitor electrodes. J Mater Chem A 5:3819–3831. https://doi.org/10.1039/C6TA04844G

Xiao C, Liu X, Mao S, Zhang LJ, Lu J (2017) Sub-micron-sized polyethylenimine-modified polystyrene/Fe₃O₄/chitosan magnetic composites for the efficient and recyclable adsorption of Cu(II) ions. Appl Surf Sci 394:378–385. https://doi.org/10.1016/j.apsusc.2016.10.116

Xing XY, Li WQ, Zhang J, Wu H, Guan Y, Gao H (2021) TEMPO-oxidized cellulose hydrogel for efficient adsorption of Cu^{2+} and Pb^{2+} modified by polyethyleneimine. Cellouse 28:7953–7968. https://doi.org/10.1007/S10570-021-04052-W

Xu Y, Wang D, Xie M, Jing L, Huang Y, Huang L, Xu H, Li H, Xie J (2019) Novel broad spectrum light responsive PPy/hexagonal-SnS₂ photocatalyst for efficient photoreduction of Cr(VI). Mater Res Bull 112:226–235. https://doi.org/10.1016/j.materresbull.2018.12.017

Zhang J, Chen H, Chen Z, He J, Shi W, Liu D, Chi H, Cui F, Wang W (2016) Microstructured macroporous adsorbent composed of polypyrrole modified natural corncob-core sponge for Cr(VI) removal. RSC Adv 6:59292–59298. https://doi.org/10.1039/C6RA07687D

Zhang L, Fang M (2010) Nanomaterials in pollution trace detection and environmental improvement. Nano Today 5:128–142. https://doi.org/10.1016/j.nantod.2010.03.002

Zhang Y, Li M, Li J, Yang Y, Liu X (2019) Surface modified leaves with high efficiency for the removal of aqueous Cr(VI). Appl Surf Sci 484:189–196. https://doi.org/10.1016/j.apsusc.2019.04.088

Zhang YZ, Zhao MW, Cheng Q, Wang C, Li HJ, Han XG, Fan ZH, Su GY, Pan D, Li ZY (2021) Research progress of adsorption and removal of heavy metals by chitosan and its derivatives: a review. Chemosphere 279:130927. https://doi.org/10.1016/J.CHEMOSPHERE.2021.130927

Zhao CH, Hu LL, Zhang CG, Wang SS, Wang XZ, Huo ZY (2021) Preparation of biochar-interpenetrated iron-alginate hydrogel as a pH-independent sorbent for removal of Cr(VI) and Pb(II). Environ Pollut 287:117303. https://doi.org/10.1016/J.ENVPOL.2021.117303

Zhao J, Li Z, Wang J, Li Q, Wang X (2015) Capsular polypyrrole hollow nanofibers: an efficient recyclable adsorbent for hexavalent chromium removal. J Mater Chem A 3:15124–15132. https://doi.org/10.1039/C5TA02525G

Publisher's Note Springer Nature remains neutral with regard to jurisdictional claims in published maps and institutional affiliations.